oceans

MDPI

Article

Seasonal Upwelling Conditions Modulate the Calcification Response of a Tropical Scleractinian Coral

Carlos E. Gómez [1,*,†], Andrés Acosta-Chaparro [1], Cesar A. Bernal [2,3], Diana I. Gómez-López [1], Raúl Navas-Camacho [1] and David Alonso [1]

[1] Programa de Biodiversidad y Ecosistemas Costeros-BEM, Instituto de Investigaciones Marinas y Costeras—INVEMAR, Santa Marta 470006, Colombia
[2] Programa de Calidad Ambiental Marina-CAM, Instituto de Investigaciones Marinas y Costeras—INVEMAR, Santa Marta 470006, Colombia
[3] Red de Investigación de Estresores Marinos—Costeros en Latinoamerica y el Caribe—REMARCO
* Correspondence: cegom.s@gmail.com
† Current address: Laboratorio de Biología Molecular Marina-BIOMMAR, Universidad de los Andes, Bogotá 111711, Colombia.

Abstract: Natural processes such as upwelling of deeper-water masses change the physical-chemical conditions of the water column creating localized ocean acidification events that can have an impact on the natural communities. This study was performed in a coral reef system of an archetypical bay within the Tayrona National Natural Park (PNNT) (Colombia), and aimed to quantify net calcification rates of a foundational coral species within a temporal context (6 months) taking into account the dynamics of seasonal upwelling that influence the study area. Net calcification rates of coral fragments were obtained in situ by the alkalinity anomaly technique in short-term incubations (~2.5 h). We found a significant effect of the upwelling on net calcification rates (*Gnet*) ($p < 0.05$) with an 42% increase in $CaCO_3$ accretion compared to non-upwelling season. We found an increase in total alkalinity (A_T) and dissolved inorganic carbon (DIC) with decreased aragonite saturation (Ω_{ara}) for the upwelling months, indicating an influence of the Subtropical Under Water mass (SAW) in the PNNT coral community. Significant negative correlations between net calcification with temperature and Ω_{ara}, which indicates a positive response of *M. auretenra* with the upwelling conditions, thus, acting as "enhancer" of resilience for coral calcification.

Keywords: carbonate chemistry; ocean acidification; coral reef; south-western Caribbean; *Madracis auretenra*

check for updates

Citation: Gómez, C.E.; Acosta-Chaparro, A.; Bernal, C.A.; Gómez-López, D.I.; Navas-Camacho, R.; Alonso, D. Seasonal Upwelling Conditions Modulate the Calcification Response of a Tropical Scleractinian Coral. *Oceans* **2023**, *4*, 170–184. https://doi.org/10.3390/oceans4020012

Academic Editors: Alma Paola Rodriguez-Troncoso, Adolfo Tortolero Langarica and Rafael Andrés Cabral-Tena

Received: 27 December 2022
Revised: 16 February 2023
Accepted: 20 March 2023
Published: 18 April 2023

1. Introduction

Coral reefs are one of the most vulnerable marine ecosystems to anthropogenic impacts, despite being classified as a key ecosystem [1]. With calcification rates in the order of 2–10 kg $CaCO_3$ m^{-2} y^{-1} [2], coral reefs constitute one of the most important bioconstructions in the world, product of the net accumulation of calcium carbonate ($CaCO_3$) of organisms such as corals and calcareous algae that are fundamental of a coral reef ecosystem [2]. The rapid increase in atmospheric CO_2 concentrations is changing the conditions in the seawater chemistry with the decrease in pH [3] and the saturation states of calcium carbonate, such as aragonite (Ω_{ara}), which is important for calcification in different coral species [4–6]. It has been estimated that by the end of the 21st century, the aragonite saturation state will shoal, exposing coral reefs around the world to corrosive waters [7,8], which increases the erosion rates, significantly altering the natural balance between accretion (calcification) and dissolution of the biogenic structures [9]. Studies from global calcification models under climate change scenarios forecast a decrease in the calcification rates of coral reefs of up to 150% by the year 2100 [2,9], with important consequences for ecosystem functioning [5,7,10].

Calcification is an important physiological process in coral reef ecosystems, and depends on species-specific functional identity, which include metabolic activity and coral morphology [11]. The formation of new calcium carbonate crystals (e.g., aragonite) occurs in a controlled environment within the organic matrix or extracellular calcification medium (ECM) [12]. To promote calcification, corals are able to up-regulate the internal carbonate chemistry within the ECM to maintain a pH and $CaCO_3$ saturation state elevated above the external environment [13–15]. Corals might also utilize bicarbonate substrate instead of carbonate as a precursor for $CaCO_3$ crystal formation as another physiological strategy that helps boots calcification in times of stressful conditions [16]. Studies have indicated that the variability in the response and the effects of ocean acidification on marine invertebrates depends on the physiological function analyzed [17]. For example, growth and calcification appears to be one of the most affected processes across organisms, and corals have showed to be among the most vulnerable due to their response to changes in the seawater carbonate chemistry [4,18–20].

Negative effects of low Ω_{ara} on calcification have been well documented for shallow-water (<20 m) [6,19,21] and cold-water corals [22,23], despite evidence of adaptation of some coral species [24–26]. Although most of the experimental work has been performed in controlled laboratory conditions, studies in CO_2 vents zones [24,27], tidal inshore reefs [19,25] and upwelling zones [28–30] provide good examples of natural laboratories for evaluating the impact of multiple co-varying factors, which will help understand the response in hypothetically future scenarios. For example, within upwelling areas, the carbonate chemistry, such as pH and aragonite saturation states, changes in response to oceanographic conditions [29–32]. In fact, large upwelling areas (Eastern Pacific) currently create ocean acidification (OA) scenarios with changes in pH of -0.1 and Ω_{ara} of -0.4 [33,34]. Moreover, there is evidence that some upwelling conditions in the Tropical Eastern Pacific (TEP) could be limiting reef development by increasing bioerosion rates and decreasing coral growth and calcification [34–36].

The shoreline of the southwestern Caribbean experiences variable and climatic and oceanographic conditions due to localized coastal upwelling [37–39]. Within the northern coast of the Colombian Caribbean, the Guajira upwelling system occurs seasonally between January and April due to the strengthening of the trade winds, where waters from ~50 to 100 m come to the surface with a decrease in mean temperature and pH [40–42]. Nutrients have been reported as low, compared to other upwelling systems [40,42]. These changes in environmental parameters are creating unique conditions in terms of water chemistry that could be affecting the coral communities that growth there. Therefore, this study aimed to answer two key questions: (1) How does carbonate chemistry vary in a reef area subjected to seasonal upwelling and (2) what is the physiological response of scleractinian corals to changes in the physical-chemical dynamics of the water column? To answer these questions, we generated a baseline of the carbonate system in the shallow reef area (13 m), as well as net calcification rates through a 6-month period in a keystone coral species in the study area.

2. Materials and Methods

Study area: This study was performed in Chengue bay within the marine protected area of the Tayrona National Natural Park (PNNT), Colombia–southwestern Caribbean Sea (11°20′ N, 74°08′ W) (Figure 1). The area is a small exemplary bay inlet (~3.3 km^2), relatively narrow, that has a diverse community of corals with coastal lagoons, marine seagrasses dominated by *Thalassia testudinum* and mangrove forest composed mainly of *Rhizophora mangle* [43]. The total percentage of live coral is about 26%, with 33% of algal cover, which has remained stable for the last decade [44]. Coral growth is restricted to a narrow band normally not exceeding 30 m. The wave protected area of the bay is dominated by species such as *Orbicella* spp., *Montastraea cavernosa*, *Pseudodiploria strigosa* and *Porites* spp., as well as extensive mono specific patches of *Madracis auretenra*. The wave exposed areas are dominated mainly by *Acropora palmata* stands [45,46].

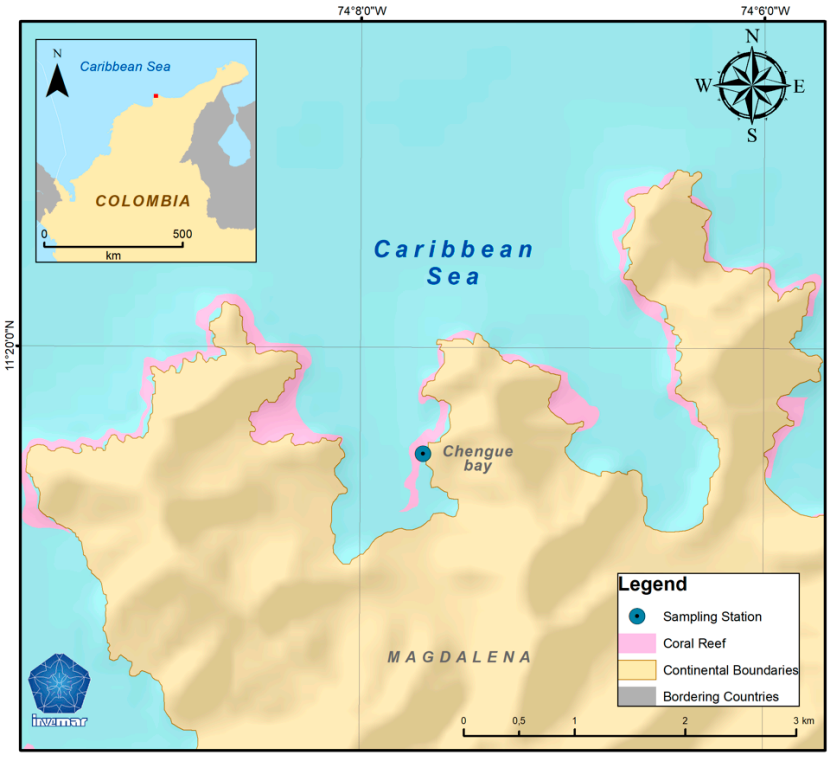

Figure 1. Map of Chengue bay within the Tayrona National Natural Park, showing the place where the incubations were performed and the discrete water samples taken for in situ characterization (dot) (insert showing the area (dot) within the Caribbean coast of Colombia) (Map source: LabSIS—INVEMAR).

The area is characterized by contrasting climatic and oceanographic conditions, mainly influenced by the northeast trade winds that cause a dry season between December and April when the winds are strong, alternated with a minor rainy season between the months of April to May and a major one between September and November [47]. In the dry season, the PNNT is influenced by an upwelling process with waters from the Subtropical Under Water (SUW) coming from depths of approximately 50 to 100 m [41,42]. This oceanographic process creates relatively cold waters (~23 °C), with increased salinity (36 psu) and lower pH (~7.9) [47,48].

Species description: *Madracis auretenra* [49] is a common zooxanthellate coral from coral reefs of the greater Caribbean Sea [50]. This species grows as dense aggregations of long, thin, dendrite-like branches, which can cover extensive areas on the substrate, such as in Santa Marta and Tayrona Park area, or grow in the form of isolated semi-hemispheric colonies [49]. This species has a wide bathymetric distribution that ranges from 2 to 60 m deep [49]. In Chengue bay, it is found distributed in the internal protected areas at a depth between 5 and 13 m [46], and its growth covers a large portion of the benthic substrate, forming structures of several square meters with almost 100% coverage (Figures S1 and S2).

In situ experimental set-up: Calcification rates of coral fragments were quantified with the alkalinity anomaly technique using custom-made incubation acrylic chambers (volume ~800 mL. Table S1). These chambers were placed in situ and secured to polyvinyl plastic quadrants (40 × 30 cm) suspended in the water column at 70 cm from the substrate with the help of foams placed on the sides of the structure, providing positive buoyancy. On each corner of the quadrant, a plastic chain attached to a lead weight kept the structure fixed on the substrate, preventing its displacement, but allowing movement from the current as "pendulant table-type" design (Figure S1). This allowed natural circulation within the chambers, in order to avoid the formation of diffusion boundary layers around the

organisms and to provide the homogeneous distribution [51,52]. The structure was located on a sandy bottom adjacent to the coral patch of *M. auretenra* at a depth of 13 m.

Carbonate chemistry analysis: Using SCUBA, discrete water samples were taken with Niskin bottles (5 L) just above the coral patch where the fragments were collected and near to the experimental set-up. Salinity and temperature data were taken at the time of water sampling with a WTW-3630 IDS conductivity–temperature probe (salinity accuracy ± 0.1; temperature accuracy ± 0.1 °C, resolution 0.1 °C). These samples were used as an initial time measurement (t_i) of total alkalinity (A_T) and dissolved inorganic carbon (DIC) in order to 1) generate the baseline of the water chemistry and 2) to obtain calcification rates of the fragments incubated inside the acrylic chambers. Water samples were collected following standard protocols [53] in 450 mL borosilicate bottles, sealed with Apiezon® grease and fixed with 100 µL of saturated mercuric chloride solution ($HgCl_2$) to prevent changes in carbonate chemistry due to biological activity [53] and stored in dark at ~21 °C for later analysis for A_T and DIC, which were performed within two to four weeks of sample collection.

A_T was determined by open cell potentiometric titration following standard protocols [54] using hydrochloric acid as titrant (0.1 mol L^{-1} HCl buffered in 0.6 mol L^{-1} NaCl, CRM Dickson Lab, Scripps Institution of Oceanography, La Jolla, California, USA). For DIC analysis, we used an automated AIRICA/Li-Cor 7000 analyzer from Marianda® following standard protocols [54]. The carbonate system was derived from total alkalinity (A_T) and dissolved inorganic carbon (DIC) using the Excel-CO2SYS program [55], taking as parameters the dissociation constant for carbonic acid from Mehrbach et al. [56], refit by Dickson & Millero [57], the constants K1 and K2 from Leuker et al. [58], $KHSO_4$ by Dickson [59] and Boron by Lee et al. [60]. These two parameters were taken as input together with temperature and salinity data to characterize pH_T (total scale), partial pressure of CO_2 in the system (µatm pCO_2), bicarbonate (HCO_3^-), carbonate concentration (CO_3^{2-}) and aragonite saturation states (Ω_{ara}). To determine the accuracy of the analysis, the samples were verified with certified reference material (CRM) for A_T and DIC, which were <0.5% estimated error (A_T: ±10 µmol kg^{-1} SW and DIC: ±3 µmol kg^{-1} SW) (Batch 171 and 190, CRM Dickson Lab, Scripps Institution of Oceanography, La Jolla, CA, USA).

Net calcification rates: To derive calcification rates from total alkalinity [61,62], four (4) sets of measurements were performed in situ from December 2020 to May 2021 (Tables 1 and S2). Each set was composed of two (2) field-work days with a total of six (6) incubations performed per day in the following way: day 1: incubations for *M. auretenra*; day 2: incubations with skeletal fragments (coral skeletons) that were carried out to determine potential dissolution rates of coral fragments only on February and March 2020, which accounts for the transition to upwelling and upwelling months. Fragments of *M. auretenra* with an average volume of 39 ± 7 cm^3 were collected on the reef between 9 and 12 m depth, and brought to the surface where they were fixed to acrylic bases with epoxy putty. The fragments on acrylic bases were then taken to the site of the experimental set-up and randomly introduced in each chamber to carry out the subsequent controlled incubations. In average, each incubation trial lasted 2.48 ± 0.43 h (Table S1). Temperature was measured in situ at 1-min intervals with a HOBO® sensor (Onset®) pendant UA-002 for the length of the trials (precision 0.14 °C, accuracy ± 0.53 °C). For each set of measurements, a control chamber without coral fragment was also incubated in order to determine possible changes in the water chemistry not related to calcification processes (e.g., microbial activity). These control values were within the range of −5 and 23 µmol kg^{-1} of seawater for total alkalinity, with respect to environmental samples, which were subtracted from the A_T of the chambers with coral fragments.

Table 1. Carbonate chemistry characterization of the study area for each of the field-work days collection and measurements. Total alkalinity (A_T), dissolved inorganic carbon (DIC), pH Total (pH_T), partial pressure of carbon dioxide (pCO_2), bicarbonate (HCO_3^-) and carbonate ions (CO_3^{2-}), and aragonite saturation (Ω_{ara}).

Date	Temp (°C)	Salinity	A_T (µmol kg^{-1})	DIC (µmol kg^{-1})	pH_T	pCO_2 (µatm)	HCO_3^-	CO_3^{2-}	Ω_{ara}
12/2/20	28.97	33.80	2369	2042	8.03	427	1796	234	3.82
12/3/20	28.87	33.70	2365	2052	8.01	452	1815	225	3.67
12/4/20	28.49	34.00	2381	2097	7.96	523	1878	206	3.35
2/17/21	26.64	35.75	2394	2069	8.03	426	1828	230	3.65
2/18/21	26.70	36.30	2383	2071	8.01	454	1838	221	3.50
2/19/21	26.00	36.29	2391	2075	8.02	436	1840	223	3.53
3/17/21	24.84	35.43	2425	2116	8.03	431	1882	221	3.50
3/18/21	25.07	35.66	2418	2113	8.02	444	1882	218	3.45
3/19/21	24.55	36.29	2416	2144	7.97	517	1933	196	3.07
5/14/21	25.89	35.08	2414	2095	8.04	422	1855	228	3.63
5/15/21	26.90	35.68	2414	2105	8.00	467	1871	221	3.52

Following the incubation time, the chambers were retrieved from the experimental set-up and brought to the surface one by one in the same order they were closed for subsequent sample collection (water and coral fragment). Once on surface, each chamber was opened and measurements of surface temperature and salinity were obtained using a WTW-3630 IDS multiparameter probe. Subsequently, the water was transferred to borosilicate bottles and fixed with $HgCl_2$ for later analysis of A_T and DIC in the laboratory (see methods in carbonate chemistry analysis). Calcification rates (*Gnet*) were quantified based on changes in total alkalinity (A_T) before and after an incubation period [61,62] using the formula:

$$Gnet = \frac{-0.5 * \Delta AT * \rho * V}{t * SA} \quad (1)$$

where ΔAT is the change in total alkalinity over the course of incubation, ρ is the density of water (kg L^{-1}), V is the chamber volume (liters), t is the incubation time (hours) and SA is the surface area of the coral fragments. Positive values of *Gnet* indicate net calcification while negative values indicate net dissolution. Net dissolution rates were measured for the transition pre-upwelling (February) and upwelling (March) using a total o 10 incubations with bare coral skeletons of the studied species with an average incubation time of 3.5 ± 0.20 h.

Statistical analysis: To test for the calcification response of *M. auretenra* in the different environmental conditions caused by the seasonal upwelling, we used the standardized calcification rates (µmol $CaCO_3$ m^{-2} h^{-1}) as the response (dependent) variable and seasons were used as independent variables using one-factor ANOVA model. The responses of individual coral fragments were grouped within each seasonal period as follow: non-upwelling—transition pre-upwelling—upwelling—transition post-upwelling. A Shapiro–Wilk test was used to test for the assumptions of normality (p = 0.112), and Levene's test for homoscedasticity (p = 0.104), which validated the assumptions of the ANOVA model. Further, to investigate the relationship between temperature and carbonate chemistry on the calcification response of *M. auretenra*, we calculated the Pearson correlation and performed regression analyses using the least-square method. For these analyses, assumption for normality of standardized residuals was checked on a histogram plot, as well as on a regression vs. the standardized predicted value to check for autocorrelation of residuals and heteroscedasticity. Results were reported as mean ± standard deviation (±s.d.) and

for all analyses, $p < 0.05$ was considered statistically significant. All statistical tests were run using R (v.4.0.3) and SPSS v.22.

3. Results

3.1. Environmental Conditions and Seawater Carbonate Chemistry at the Sampling Site

Temperature and salinity showed variations between the sampling months. We observed a decrease in the mean temperature from 28.27 ± 0.11 °C for the month of December (non-upwelling) to 24.75 ± 0.17 °C corresponding to March 2021 (upwelling) (Table 1, Figure 2). This decrease in temperature was coincident with increase in wind velocity within the area due to the north-west trade winds (Figure 3). Likewise, we observed an increase in salinity from 33.49 ± 0.21 in December to around 36 for the following months (Table 1).

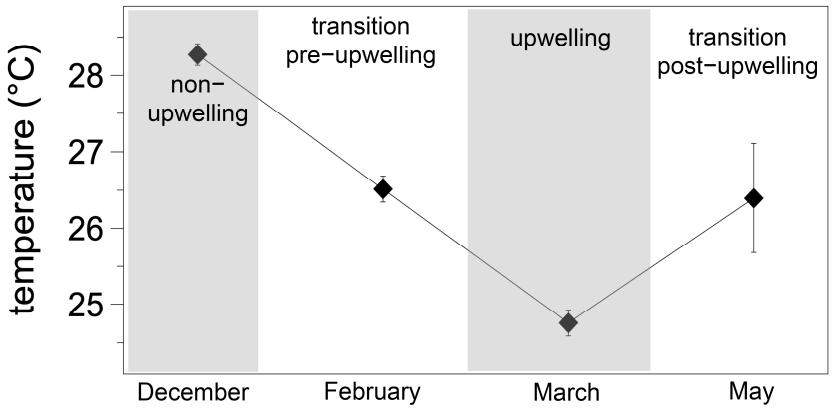

Figure 2. Mean temperature (±s.d.) for each of the field-work days when the incubations were performed.

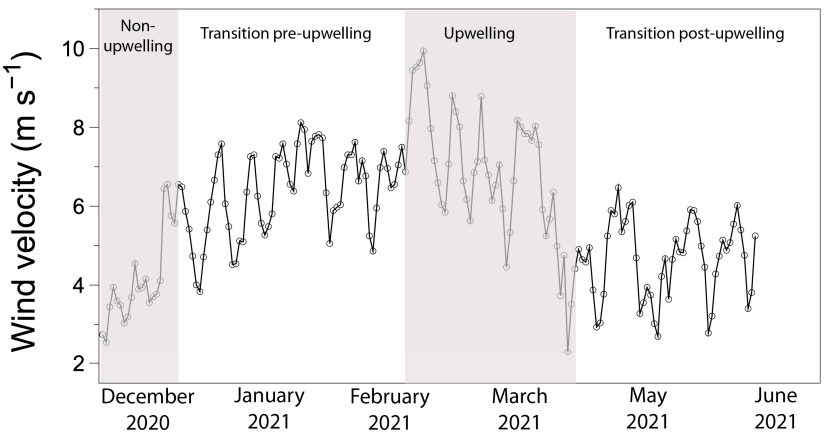

Figure 3. Wind velocity for the Santa Marta area between December 2020 and May 2021. Data were taken from Windguru (www.windguru.com, accessed on 15 March 2022) and correspond to values from the climatological station located at the Simón Bolivar international airport (lat: 11.1548, lon: −74.2264, alt: 6 m).

Seawater chemistry values showed variation during the sampling months, particularly for total alkalinity and DIC that increased approximately 2.5% during the upwelling season from 2371 ± 8 to 2419 ± 5 µmol kg^{-1} SW and 2063 ± 29 to 2124 ± 17 µmol kg^{-1} SW, respectively. Significant correlations were found between temperature and A_T (Pearson: −0.88, R^2: 0.78, $p < 0.01$), temperature and DIC (Pearson: −0.78, R^2: 0.61, $p < 0.01$), and temperature and bicarbonate ion (HCO_3^-) (Pearson: −0.71, R^2: 0.50, $p < 0.05$). Although, we did not find any significant correlations between temperature and the other seawater chemistry parameters, we observed that average Ω_{ara} decreased from 3.82 ± 0.24 to 3.34 ± 0.23

with values dropping as low as 3.07 during upwelling season. Despite these changes, other parameters in the carbonate chemistry showed little seasonal variation (Table 2).

Table 2. Environmental variables, temperature in Celsius (Temp°C) and salinity. Total alkalinity before the incubations (A_T(i)), total alkalinity after the incubations (A_T(f)), net calcification (*Gnet*) and net dissolution. Measurements denoted by [——.——] were not performed in those dates. Values are given as mean ± s.d.

Season	Date	*n*	Temp (°C)	Salinity	$A_{T(i)}$ (µmol kg^{-1} SW)	$A_{T(f)}$ (µmol kg^{-1} SW)	*Gnet* (µmol $CaCO_3$ m^{-2} h^{-1})	Dissolution (µmol $CaCO_3$ m^{-2} h^{-1})
non-upwelling	12/2/20	5	29.0 ± 0.4	33.3 ± 0.2	2369	2313 ± 34	27.7 ± 4.8	——.——
	12/3/20	5	28.9 ± 0.2	33.4 ± 0.1	2364	2325 ± 42	19.9 ± 7.8	——.——
transition pre-upwelling	2/17/21	5	26.6 ± 0.01	35.9 ± 0.1	2394	2304 ± 57	25.2 ± 5.4	——.——
	2/19/21	5	26.1 ± 0.01	36.1 ± 0.2	2391	2385 ± 11	——.——	3.1 ± 4.6
upwelling	3/17/21	5	24.8 ± 0.01	35.5 ± 0.4	2425	2270 ± 83	41.8 ± 11.6	——.——
	3/19/21	5	25.1 ± 0.01	36.3 ± 0.1	2415	2429 ± 24	——.——	−5.6 ± 10.7
transition post-upwelling	5/14/21	5	26.1 ± 0.01	35.98 ± 0.22	2414	2311 ± 66	32.5 ± 6.9	——.——

3.2. Calcification and Dissolution Rates

In total, we incubated 25 independent living coral fragments of *M. auretenra* throughout the sampling months (December: $n = 10$; February: $n = 5$; March: $n = 5$; May: $n = 5$ fragments). We observed significant changes between seasons (ANOVA, $F_{2,25} = 6.395$ $p = 0.003$, Figure 4, Table 3), with a ~42% increase in the calcification rates in upwelling compared to non-upwelling and transition pre-upwelling (post-hoc Tukey HSD, Table 3). On average, net calcification rates for non-upwelling was 23.8 ± 7.3 µmol $CaCO_3$ m^{-2} h^{-1} with a range between 8 and 35 µmol CaCO3 m^{-2} h^{-1}. For the transition periods (pre-upwelling and post-upwelling), average net calcification was 25.2 ± 5.4 and 32.5 ± 6.9 µmol $CaCO_3$ m^{-2} h^{-1}, respectively, and for upwelling season (March), average net calcification was 41.8 ± 11.6 µmol $CaCO_3$ m^{-2} h^{-1}, ranging between 33 and 51 µmol CaCO3 m^{-2} h^{-1} (Figure 4). We found a significant correlation between calcification and temperature (Pearson = −0.62, $R^2 = 0.38$, $p < 0.01$) and calcification and aragonite saturation (Ω_{ara}) (Pearson = −0.44, $R^2 = 0.21$, $p < 0.05$) (Figure 5A,B), with higher values corresponding to a decrease in temperature and Ω_{ara}. Dissolution rates during the upwelling averaged −5.6 ± 10.7 µmol $CaCO_3$ m^{-2} h^{-1}, while for the transition period (February), values averaged 3.1 ± 4.6 µmol $CaCO_3$ m^{-2} h^{-1} (Table 2).

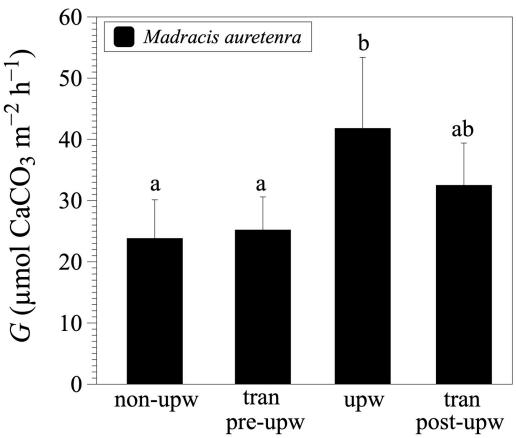

Figure 4. Net calcification rates (mean ± s.d.) for coral fragments of *M. auretenra* incubated in situ according to the different field-work seasons. Non-upwelling season (non-upw)-December, transition pre-upwelling season (tran pre-upw)-February, peak upwelling season (upw)-March, transition post-upwelling season (tran post-upw)-May. Letters a and b denote significant differences ($p < 0.05$).

Table 3. ANOVA results showing the probability values for treatment differences (seasons) and post hoc test that corresponds to: non-upwelling season (non-upw)-December, transition pre-upwelling season (tran pre-upw)-February, peak upwelling season (upw)-March, transition post-upwelling season (tran post-upw)-May.

Source	Type-III Sum Squares	df	Mean Squares	F	Sig
Treatment	1212.13	2	404.046	6.395	0.003
Error	1326.711	21	63.177		
Total	24,170.51	25			
Post-Hoc Tukey HSD					
Treatment	non-upw	tran pre-upw	upw	tran post-upw	
non-upw	—-.—-	0.989	0.003	0.223	
tran pre-upw	0.989	—-.—-	0.017	0.482	
upw	0.003	0.017	—-.—-	0.281	
tran post-upw	0.223	0.482	0.281	—-.—-	

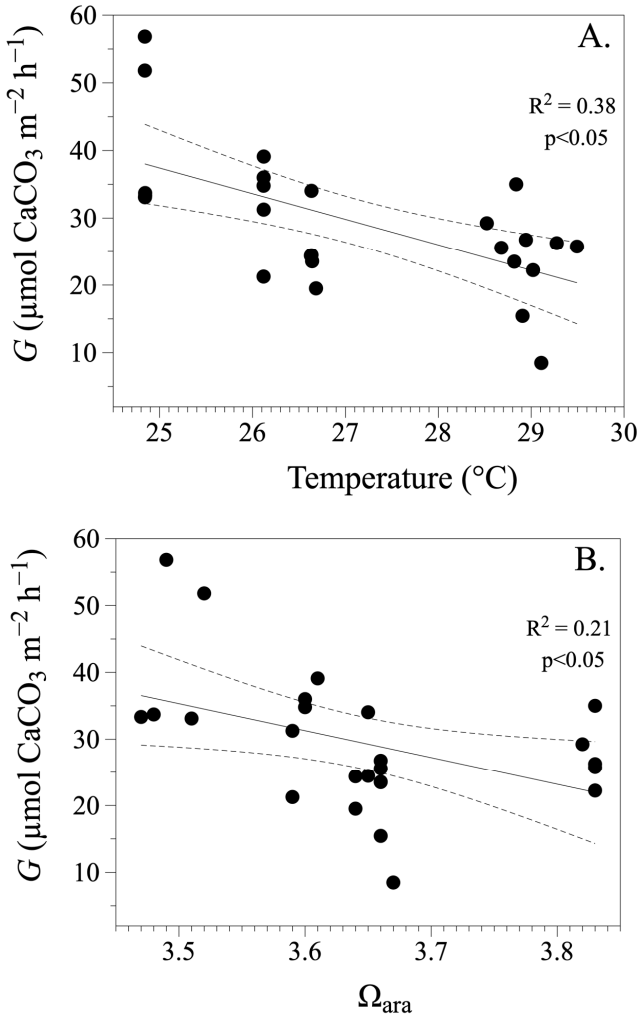

Figure 5. Correlation plots between (**A**) temperature vs. net calcification and (**B**) Ω_{ara} vs. net calcification of fragment of *M. auretenra*.

4. Discussion

Localized upwelling events caused changes in net calcification of *Madracis auretenra* due to natural variability in environmental conditions commonly experienced in the study area. Mean temperature changes of ~5 °C (from 29 °C to 24 °C) and Ω_{ara} of ~0.5 (from 3.82 to 3.34) characterized the upwelling, which came by pulses from January through March with clear periods of relaxation/intensification mainly driven by the strengthening of the trade winds (>10 m s^{-2}). From mid-December to mid-February 2020, we observed a period of transitioning to upwelling, then an intensification during February to March and transitioning to non-upwelling conditions again from mid-April to May 2020. As seen in the present study and in accordance with other studies using satellite images of SST (AVHRR) [37], the main cooling event occurs during January–April, with 2 to 4 upwelling pulses and a maximum detected during February–March.

Upwelling and its influence in the carbonate chemistry dynamics: Upwelling conditions in the Colombian Caribbean during the dry season include cold surface waters (21–24 °C), high salinity (>35 ups) and oxygen saturation <90% in the surface layers [41,42,63]. We observed temperatures ~28–29 °C and salinity ~34 for December when the upwelling had not happened, which indicates the presence of a stratified water column of the Caribbean Surface Waters (CSW) within the area [41]. This water mass is characteristic at depths shallower than 30 m predominant in the non-upwelling months (e.g., December in this study) [41]. For the months that followed the transition and peak upwelling conditions, temperature dropped to 24 °C and salinity increased to ~36. These conditions were created by the influence of the Subtropical Underwater Mass (SUW) that upwell from a depth of about 50 to 100 m, and is characteristic of the Guajira upwelling system [41,42]. Andrade and Barton [40] suggest that the subsurface waters that supply the upwelling system in La Guajira may be influenced by a coastal branch from the Panama-Colombia Gyre, whose surface origin and moderately young waters determines its physical-chemical characteristics, as well as its lower nutrient concentration (e.g., [48]) compared to other upwelling centers within the southern Caribbean upwelling systems [37].

We observed an increase in total alkalinity (A_T) and dissolved inorganic carbon (DIC) during upwelling months. Although, these results are baseline data measured for the Tayrona area, we found that are within the reported values for a similar upwelling system (Cariaco Basin, Venezuela) that has been subject of different studies focused on the carbonate chemistry [64–66]. During the peak upwelling (February–March) we found values > 2400 µmol kg^{-2} for A_T and >2100 µmol kg^{-2} for DIC, which explained the chemical nature of the upwelling and the SUW in the area [66,67]. The little variation in pCO_2 (from 453 to 456) and pH_T (~8.01) may be related to the relatively shallow-water mass that upwell within the study area, which may not create considerable changes in these carbonate chemistry variables due to its young age [40]. Other factors associated to metabolic pulses (respiration–photosynthesis and calcification–dissolution) and water mass residence time within shallow-water coral reef areas, have the ability to influence the local carbonate chemistry creating a "buffer" effect raising the levels of CO_2 and pH_T [68,69]. It is important to note that discrete water samples for carbonate chemistry measurements were taken just above the reef (~1.5 m) and not at the surface or at different depths in the water column; thus, it is necessary to carry out specific studies to be able to answer these questions related to buffer effect in this particular reef system.

Calcification under seasonal upwelling: Seasonal differences in temperature and Ω_{ara} had a main effect on the calcification rate of *M. auretenra*. Net calcification increased by 42% under upwelling when temperature and Ω_{ara} were lower with average values of 41.8 ± 11.7 µmol $CaCO_3$ m^{-2} h^{-1} for upwelling season compared to 23.8 ± 7.3 µmol $CaCO_3$ m^{-2} h^{-1} for non-upwelling. Both variables, temperature and Ω_{ara}, have been central in the study of climate change, since both have the capacity to alter metabolic functions [21]. Although comparisons with other studies are variable and depends on multiple factors, such as type of coral growth and method employed to measure calcification, as well as community vs. single species approach [11,70], our results indicate that the average

net calcification rates for ambient conditions are in agreement with other studies using similar approach and working with the same coral species [16].

When comparing physiological response of marine calcifiers (calcification rates, metabolic functions) with other studies performed in other upwelling areas (e.g., eastern Pacific, northern Arabian Sea), there is the consensus that changes in the carbonate chemistry variables such as decreased temperature, pH_T and Ω_{ara}, exert strong effect on functional performance [29–31]. For example, seasonal upwelling in the Indian Ocean, which had values of Ω_{ara} ranging from ~4 to ~3.2 [30], exert a negative response in the extension and calcification rates of *Porites* sp., similar to what has been found on Pocilloporid corals from the Gulf of Panama [71]. One plausible explanation is that elevated primary productivity in upwelling season is causing a loss in photosynthetic efficiency that is reflected in the decrease in calcification rates and linear extension [30], which might also apply to corals in the Tayrona area, where nutrient concentrations are lower than other more productive upwelling systems [40,48].

We found that calcification rates had a negative function with respect to temperature and Ω_{ara}, despite different studies performed to date that have concluded that calcification is a positive function of temperature and carbonate ion concentration (CO_3^{2-}) [6,9,72–76]. The upwelling-induced counteractive mechanism observed in the present study in the calcification of *M. auretenra* might be explained in part from the holobiont internal carbonate chemistry control, as has been shown in other studies working with tropical scleractinian corals. As oceans become more acidic, mechanisms of coral calcification to counteract the carbonate depletion involve pH up-regulation, in which corals are able to control the internal chemistry of the calcifying space [13], and switching from CO_3^{2-} to HCO_3^- as the primary substrate for $CaCO_3$ deposition [16,77,78]. Although we found a significant positive correlation between net calcification and bicarbonate ion concentration [HCO_3^-] (Pearson: 0.61, $R^2 = 0.37$, $p < 0.01$), the relative contribution of increased bicarbonate at constant CO_3^{2-} was not measured in the present study. One study performed on *M. auretenra*, indicates that this species responds more to [HCO_3^-] than to [CO_3^{2-}], thus giving this species resistance to OA [16]. To date, this is the only evidence, despite other studies having found opposite results [74,76]. Moreover, studies using in situ approach indicated that calcification rates are dependent on the Ω_{ara}, with approximately 52% reduction per unit decrease in saturation state, even in coral species considered tolerant to changes in environmental conditions [79]. Another scenario with counteractive response will favor coral calcification and growth due to increments in DIC that has been shown to enhance photosynthetic efficiency, thus physiological performance [80].

Ecological implications: Global models for ocean acidification indicate a decrease in the saturation state of calcium carbonate, particularly aragonite, important precursor for coral calcification [7], and can be more accentuated in areas naturally experiencing changing environmental conditions such as upwelling systems [33]. However, the success and persistence of *M. auretenra* in the study area is an example of adaptability of a scleractinian coral to natural variability in ecological and physiological conditions. Over the course of this study, changes in seawater chemistry, particularly Ω_{ara} at Chengue bay, remained adequately to marginally saturated (from ~3.8 to ~3.3), the pH_T remained above 8.00 for >95% of the time except one measurement performed in March that we recorded 7.96 (Table 2), and pCO_2 was within the average for current ambient atmospheric values (420–450 µatm). This means that a moderate upwelling such as the one in PNNT benefits the coral community and could potentially act as refuge for climate change in general. For example, ecological studies performed within the Tayrona area indicated that bleaching susceptibility of corals is lower than in other areas of coral reefs in the South-Western Caribbean due, presumably, to the cooling effect caused by the upwelling processes [48]. Moreover, when bleaching was relatively high within the area, corals recovered quickly during the upwelling, indicating local resilience against climate change stressor [48,81,82]. Ecological restoration studies have been modelling artificially-generated upwelling conditions to see if it can effectively reduce sea surface temperature (SST) and degree heating weeks (DHW), and slow future

coral bleaching events [83,84]. Future research should evaluate the calcification response in different climate change scenarios in order to test hypothesis concerning adaptability and resilience not only of *M. auretenra*, but also comparing it with conspecifics from the nearby reefs.

5. Conclusions

This study showed that variables of the carbonate chemistry system varied according to seasonal upwelling. These results represent a key baseline input for future studies on carbonate chemistry and ocean acidification for the area. Differences were found in surface temperature, salinity and some variables of the carbonate system such as A_T, DIC, HCO_3^- and Ω_{ara}. The other parameters remained relatively homogeneous during the sampling period, such as pCO_2 and pH_T, opposite to the patterns expected for an upwelling system. The pattern may be explained by the physical nature of the upwelling, which emerges from a shallow water mass (50–100 m) on the Colombian Caribbean coast. Net calcification (*Gnet*) of *M. auretenra*, which increased for the upwelling period, was significantly correlated to temperature and Ω_{ara}. It is worth pointing out that there are still covarying factors affecting these correlations, since about 62% and 79% other than temperature and aragonite, respectively, are affecting calcification rates. Nevertheless, these results still indicate negative feedback in the physiological response where *M. auretenra* is able to control calcification to counteract changes in temperature and carbonate chemistry. Many questions remain unanswered associated with different physical (geomorphology, residence time and water exchange within the bay) as well as biological factors such as metabolic pulses (respiration/photosynthesis—calcification/dissolution) that can have an external buffer effect on the reef. Moreover, we did not differentiate between the relative effects of day and night calcification vs. respiration and photosynthesis, which will account for the calcium carbonate budget that should be included in future studies.

Supplementary Materials: The following supporting information can be downloaded at: https://www.mdpi.com/article/10.3390/oceans4020012/s1, Figure S1. Experimental design in Chengue bay. (A) incubation chambers within the pendulant table-type design, (B) fragment close-up showing the natural appearance of the extend polyps during incubation trials, and (C) deployment of the chamber by divers. Figure S2. Coral reef in Chengue bay where the main growth of M. auretenra were found. Table S1. Raw data for each of the incubation fragments (replicates). Temperature (Temp) in celcius, salinity (Sal) in practical salinity units (PSU), chamber volume (net), fragment volume, depth (meters) and incubation time (minutes). Table S2. Raw data for each of the incubation fragments (replicates). Total alkalinity (A_T—μmol $CaCO_3$ m^2 h^{-1}) initial (i) and final (f), dissolved inorganic carbon (DIC—μmol $CaCO_3$ m^2 h^{-1}) initial (i) and final (f), net calcification (G—μmol $CaCO_3$ m^2 h^{-1}) and net dissolution (μmol $CaCO_3$ m^2 h^{-1}).

Author Contributions: Conceptualization, C.E.G., D.A., C.A.B. and D.I.G.-L.; methodology, C.E.G., A.A.-C., C.A.B. and R.N.-C.; formal analysis, C.E.G.; investigation, C.E.G., A.A.-C., C.A.B., D.I.G.-L. and R.N.-C.; resources, C.E.G., D.A., C.A.B. and D.I.G.-L.; data curation, C.E.G.; writing—original draft preparation, C.E.G.; writing—review and editing, C.E.G., A.A.-C., D.A., C.A.B., D.I.G.-L. and R.N.-C. All authors have read and agreed to the published version of the manuscript.

Funding: This research was funded by the Colombian Ministry of Science—MINCIENCIAS grant number 848-2019 within the program "Estancias Postdoctorales en entidades del SNCT" and Instituto de Investigaciones Marinas y Costeras (INVEMAR) through the project "Investigación científica hacia la generación de información y conocimiento de las zonas marinas y costeras de interés de la nación", BPIN code 2017011000113. This is a contribution # 1354 from INVEMAR.

Institutional Review Board Statement: Not applicable.

Informed Consent Statement: Not applicable.

Data Availability Statement: Raw data from this study is available within the Supplementary Materials.

Acknowledgments: Special thanks to María del Pilar Parrado, Laura Sánchez and Juan David Gonzalez who provided technical support in the field; Catalina Arteaga and Miguel Martelo from the MHNMC provided logistic resources; and Karen Ibarra and Gustavo Lara for laboratory technical support (LABCAM) and LabSIS-Invemar. Thanks to Cecil Bolaños, Daniel Parra, Eduardo Vilarete and Eduardo Jaraba for technical assistance during field work. We would like to thank two anonymous reviewers for their constructive comments on this manuscript.

Conflicts of Interest: The authors declare no conflict of interest. The funders had no role in the design of the study; in the collection, analyses, or interpretation of data; in the writing of the manuscript; or in the decision to publish the results.

References

1. Hoegh-Guldberg, O.; Bruno, J.F. The impact of climate change on the world's marine ecosystems. *Science* **2010**, *328*, 1523–1528. [CrossRef]
2. Cornwall, C.E.; Comeau, S.; Kornder, N.A.; Perry, C.T.; van Hooidonk, R.; DeCarlo, T.; Pratchett, M.S.; Anderson, K.D.; Brown, N.; Carpenter, R.; et al. Global declines in coral reef calcium carbonate production under ocean acidification and warming. *Proc. Natl. Acad. Sci. USA* **2021**, *118*, e2015265118. [CrossRef]
3. Caldeira, K.; Wickett, M.E. Anthropogenic carbon and ocean pH. *Nature* **2003**, *425*, 365. [CrossRef]
4. Gattuso, J.; Frankignoulle, M.; Bourge, I.; Romaine, S.; Buddemeier, R.W. Effect of calcium carbonate saturation of seawater on coral calcification. *Glob. Planet. Change* **1998**, *18*, 37–46. [CrossRef]
5. Kleypas, J.A.; Buddemeier, R.W.; Archer, D.; Gattuso, J.P.; Langdon, C.; Opdyke, B.N. Geochemical consequences of increased atmospheric carbon dioxide on coral reefs. *Science* **1999**, *284*, 118–120. [CrossRef]
6. Langdon, C.; Atkinson, M.J. Effect of elevated pCO_2 on photosynthesis and calcification of corals and interactions with seasonal change in temperature/irradiance and nutrient enrichment. *J. Geophys. Res.* **2005**, *110*, C09S07. [CrossRef]
7. Orr, J.C.; Fabry, V.J.; Aumont, O.; Bopp, L.; Doney, S.C.; Feely, R.A.; Gnanadesikan, A.; Gruber, N.; Ishida, A.; Joos, F.; et al. Anthropogenic ocean acidification over the twenty-first century and its impact on calcifying organisms. *Nature* **2005**, *437*, 681–686. [CrossRef]
8. Guinotte, J.M.; Orr, J.; Cairns, S.; Freiwald, A.; Morgan, L.; George, R. Will human-induced changes in seawater chemistry alter the distribution of deep-sea scleractinian corals? *Front. Ecol. Environ.* **2006**, *4*, 141–146. [CrossRef]
9. Eyre, B.D.; Cyronak, T.; Drupp, P.; De Carlo, E.H.; Sachs, J.P.; Andersson, A.J. Coral reefs will transition to net dissolving before end of century. *Science* **2018**, *359*, 908–911. [CrossRef]
10. Feely, R.A.; Sabine, C.L.; Lee, K.; Berelson, W.; Kleypas, J.; Fabry, V.J.; Millero, F.J. Impact of anthropogenic CO_2 on the $CaCO_3$ system in the oceans. *Science* **2004**, *305*, 362–366. [CrossRef]
11. González-Barrios, F.J.; Álvarez-Filip, L. A framework for measuring coral species-specific contribution to reef functioning in the Caribbean. *Ecol. Indic.* **2018**, *95*, 877–886. [CrossRef]
12. Allemand, D.; Ferrier-Pagès, C.; Furla, P.; Houlbrèque, F.; Puverel, S.; Tambutté, R.E.; Tambutté, S.; Zoccola, D. Biomineralisation in reef-building corals: From molecular mechanisms to environmental control. *Comptes. Rendus. Palevol.* **2004**, *3*, 453–467. [CrossRef]
13. McCulloch, M.; Falter, J.; Trotter, J.; Montagna, P. Coral resilience to ocean acidification and global warming through pH up-regulation. *Nat. Clim. Change* **2012**, *2*, 623–627. [CrossRef]
14. Holcomb, M.; Venn, A.A.; Tambutté, E.; Tambutté, S.; Allemand, D.; Trotter, J.; Mcculloch, M. Coral calcifying fluid pH dictates response to ocean acidification. *Sci. Rep.* **2015**, *4*, 5207. [CrossRef] [PubMed]
15. Raybaud, V.; Tambutté, S.; Ferrier-Pagès, C.; Reynaud, S.; Venn, A.A.; Tambutté, É.; Nival, P.; Allemand, D. Computing the carbonate chemistry of the coral calcifying medium and its response to ocean acidification. *J. Theor. Biol.* **2017**, *424*, 26–36. [CrossRef] [PubMed]
16. Jury, C.P.; Whitehead, R.F.; Szmant, A.M. Effects of variations in carbonate chemistry on the calcification rates of *Madracis auretenra* (=*Madracis mirabilis sensu* Wells, 1973): Bicarbonate concentrations best predict calcification rates. *Glob. Change Biol.* **2010**, *16*, 1632–1644. [CrossRef]
17. Leung, J.Y.S.; Zhang, S.; Connell, S.D. Is Ocean acidification really a threat to marine calcifiers? A systematic review and meta-analysis of 980+ studies spanning two decades. *Small* **2022**, *18*, 2107407. [CrossRef]
18. Hoegh-Guldberg, O.; Mumby, P.J.; Hooten, A.J.; Steneck, R.S.; Greenfield, P.; Gomez, E.; Harvell, C.D.; Sale, P.F.; Edwards, A.J.; Caldeira, K.; et al. Coral reefs under rapid climate change and ocean acidification. *Science* **2007**, *318*, 1737–1742. [CrossRef]
19. Albright, R.; Takeshita, Y.; Koweek, D.A.; Ninokawa, A.; Wolfe, K.; Rivlin, T.; Nebuchina, Y.; Young, J.; Caldeira, K. Carbon dioxide addition to coral reef waters suppresses net community calcification. *Nature* **2018**, *555*, 516–519. [CrossRef]
20. Kroeker, K.J.; Kordas, R.L.; Crim, R.; Hendriks, I.E.; Ramajo, L.; Singh, G.S.; Duarte, C.M.; Gattuso, J.P. Impacts of ocean acidification on marine organisms: Quantifying sensitivities and interaction with warming. *Glob. Change Biol.* **2013**, *19*, 1884–1896. [CrossRef]
21. Kroeker, K.J.; Kordas, R.L.; Crim, R.N.; Singh, G.G. Meta-analysis reveals negative yet variable effects of ocean acidification on marine organisms: Biological responses to ocean acidification. *Ecol. Lett.* **2010**, *13*, 1419–1434. [CrossRef] [PubMed]

22. Hennige, S.J.; Wicks, L.C.; Kamenos, N.A.; Perna, G.; Findlay, H.S.; Roberts, J.M. Hidden impacts of ocean acidification to live and dead coral framework. *Proc. R. Soc. B* **2015**, *282*, 20150990. [CrossRef] [PubMed]
23. Gómez, C.E.; Wickes, L.; Deegan, D.; Etnoyer, P.J.; Cordes, E.E. Growth and feeding of deep-sea coral *Lophelia pertusa* from the California margin under simulated ocean acidification conditions. *PeerJ* **2018**, *6*, e5671. [CrossRef] [PubMed]
24. Fabricius, K.E.; Langdon, C.; Uthicke, S.; Humphrey, C.; Noonan, S.; De'ath, G.; Okazaki, R.; Muehllehner, N.; Glas, M.S.; Lough, J.M. Losers and winners in coral reefs acclimatized to elevated carbon dioxide concentrations. *Nat. Clim. Change* **2011**, *1*, 165–169. [CrossRef]
25. Kurihara, H.; Watanabe, A.; Tsugi, A.; Mimura, I.; Hongo, C.; Kawai, T.; Reimer, J.D.; Kimoto, K.; Gouezo, M.; Golbuu, Y. Potential local adaptation of corals at acidified and warmed Nikko Bay, Palau. *Sci. Rep.* **2021**, *11*, 11192. [CrossRef]
26. Glazier, A.; Herrera, S.; Weinnig, A.; Kurman, M.; Gómez, C.E.; Cordes, E. Regulation of ion transport and energy metabolism enables certain coral genotypes to maintain calcification under experimental ocean acidification. *Mol. Ecol.* **2020**, *29*, 1657–1673. [CrossRef]
27. Hall-Spencer, J.M.; Rodolfo-Metalpa, R.; Martin, S.; Ransome, E.; Fine, M.; Turner, S.M.; Rowley, S.J.; Tedesco, D.; Buia, M.C. Volcanic carbon dioxide vents show ecosystem effects of ocean acidification. *Nature* **2008**, *454*, 96–99. [CrossRef]
28. Enochs, I.C.; Manzello, D.P.; Kolodziej, G.; Noonan, S.H.; Valentino, L.; Fabricius, K.E. Enhanced macroboring and depressed calcification drive net dissolution at high-CO_2 coral reefs. *Proc. R. Soc. B* **2016**, *283*, 20161742. [CrossRef]
29. Sánchez-Noguera, C.; Stuhldreier, I.; Cortés, J.; Jiménez, C.; Morales, Á.; Wild, C.; Rixen, T. Natural Ocean acidification at Papagayo upwelling system (north Pacific Costa Rica): Implications for reef development. *Biogeosciences* **2018**, *15*, 2349–2360. [CrossRef]
30. Spreter, P.M.; Reuter, M.; Mertz-Kraus, R.; Taylor, O.; Brachert, T.C. Calcification response of reef corals to seasonal upwelling in the northern Arabian Sea (Masirah Island, Oman). *Biogeosciences* **2022**, *19*, 3559–3573. [CrossRef]
31. Ramajo, L.; Valladares, M.; Astudillo, O.; Fernández, C.; Rodríguez-Navarro, A.B.; Watt-Arévalo, P.; Núñez, M.; Grenier, C.; Román, R.; Aguayo, P.; et al. Upwelling intensity modulates the fitness and physiological performance of coastal species: Implications for the aquaculture of the scallop *Argopecten purpuratus* in the Humboldt Current System. *Sci. Total Environ.* **2020**, *745*, 140949. [CrossRef] [PubMed]
32. Feely, R.A.; Sabine, C.L.; Hernandez-Ayon, J.M.; Ianson, D.; Hales, B. Evidence for upwelling of corrosive 'acidified' water onto the continental shelf. *Science* **2008**, *320*, 1490–1492. [CrossRef] [PubMed]
33. Gruber, N.; Hauri, C.; Lachkar, Z.; Loher, D.; Frölicher, T.L.; Plattner, G.K. Rapid progression of ocean acidification in the California Current System. *Science* **2012**, *337*, 220–223. [CrossRef]
34. Manzello, D.P. Coral growth with thermal stress and ocean acidification: Lessons from the eastern tropical Pacific. *Coral Reefs* **2010**, *29*, 749–758. [CrossRef]
35. Manzello, D.P.; Kleypas, J.A.; Budd, D.A.; Eakin, C.M.; Glynn, P.W.; Langdon, C. Poorly cemented coral reefs of the Eastern Tropical Pacific: Possible insights into reef development in a high-CO_2 world. *Proc. Natl. Acad. Sci. USA* **2008**, *105*, 10450–10455. [CrossRef]
36. Glynn, P.W.; Alvarado, J.J.; Banks, S.; Cortés, J.; Feingold, J.S.; Jiménez, C.; Maragos, J.E.; Martínez, P.; Maté, J.L.; Moanga, D.A.; et al. Eastern Pacific coral reef provinces, coral community structure and composition: An overview. In *Coral Reefs of the Eastern Tropical Pacific*; Glynn, P.W., Manzello, D.P., Enochs, I.C., Eds.; Springer: Amsterdam, The Netherlands, 2017; Volume 8, pp. 107–176.
37. Rueda-Roa, D.T.; Muller-Karger, F.E. The southern Caribbean upwelling system: Sea surface temperature, wind forcing and chlorophyll concentration patterns. *Deep. Sea Res. Part I Oceanogr. Res. Pap.* **2013**, *78*, 102–114. [CrossRef]
38. Rueda-Roa, D.; Ezer, T.; Muller-Karger, F. Description and mechanisms of the mid-year upwelling in the Southern Caribbean Sea from remote sensing and local data. *JMSE* **2018**, *6*, 36. [CrossRef]
39. Santos, F.; Gómez-Gesteira, M.; Varela, R.; Ruiz-Ochoa, M.; Días, J.M. Influence of upwelling on SST trends in La Guajira system. *J. Geophys. Res. Oceans* **2016**, *121*, 2469–2480. [CrossRef]
40. Andrade, C.A.; Barton, E.D. The Guajira upwelling system. *Cont. Shelf Res.* **2005**, *25*, 1003–1022. [CrossRef]
41. Paramo, J.; Correa, M.; Núñez, S. Evidencias de desacople físico-biológico en el sistema de surgencia en La Guajira, Caribe colombiano. *Rev. Biol. Mar. Oceanogr.* **2011**, *46*, 421–430. [CrossRef]
42. Correa-Ramirez, M.; Rodriguez-Santana, Á.; Ricaurte-Villota, C.; Paramo, J. The Southern Caribbean upwelling system off Colombia: Water masses and mixing processes. *Deep Sea Res. Part I Oceanogr. Res. Pap.* **2020**, *155*, 103145. [CrossRef]
43. Garzón-Ferreira, J. Bahía de Chengue, Parque Nacional Natural Tayrona, Colombia. In *Caribbean Coral Reef, Seagrass and Mangrove Sites*; Unesco: Paris, France, 1998; pp. 115–125.
44. Gómez-López, D.I.; Acosta-Chaparro, A.; Gonzalez, J.D.; Sanchez, L.; Navas-Camacho, R.; Alonso, D. *Reporte del Estado de Los Arrecifes Coralinos y PASTOS marinos en Colombia (2016–2017)*; Serie de Publicaciones Generales del Invemar #101; INVEMAR: Santa Marta, Colombia, 2018; 100p.
45. Garzón-Ferreira, J.; Díaz, J.M. The Caribbean coral reefs of Colombia. In *Latin American Coral Reefs*; Cortés, J., Ed.; Elsevier: Amsterdam, The Netherlands, 2003; pp. 275–301. [CrossRef]
46. Díaz, J.M.; Barrios, L.M.; Cendales, M.H.; Garzón-Ferreira, J.; Geister, J.; López-Victoria, M.; Ospina, G.; Parra-Velandia, F.; Pinzón, J.; Vargas-Angel, B.; et al. *Áreas Coralinas de Colombia*; Serie Publicaciones Especiales No. 5; INVEMAR: Santa Marta, Colombia, 2000; p. 176.

47. Arévalo-Martínez, D.L.; Franco Herrera, A. Características oceanográficas de la surgencia frente a la ensenada de Gaira, Departamento de Magdalena, época seca menor de 2006. *Bol. Inv. Mar. Cost.* **2016**, *37*, 131–162. [CrossRef]
48. Bayraktarov, E.; Pizarro, V.; Wild, C. Spatial and temporal variability of water quality in the coral reefs of Tayrona National Natural Park, Colombian Caribbean. *Environ. Monit. Assess.* **2014**, *186*, 3641–3659. [CrossRef]
49. Locke, J.M.; Weil, E.; Coates, K.A. A newly documented species of *Madracis* (Scleractinia: Pocilloporidae) from the Caribbean. *Proc. Biol. Soc. Wash.* **2007**, *120*, 214–226. [CrossRef]
50. Sebens, K.P.; Witting, J.; Helmuth, B. Effects of water flow and branch spacing on particle capture by the reef coral *Madracis mirabilis* (Duchassaing and Michelotti). *J. Exp. Mar. Biol. Ecol.* **1997**, *211*, 1–28. [CrossRef]
51. Hurd, C.L. Water motion, marine macroalgal physiology, and production. *J. Phycol* **2000**, *36*, 453–472. [CrossRef]
52. Carvalho, V.F.; Silva, J.; Kerr, R.; Anderson, A.B.; Bastos, E.O.; Cabral, D.; Gouvêa, L.P.; Peres, L.; Martins, C.D.L.; Silveira-Andrade, V.M.; et al. When descriptive ecology meets physiology: A study in a South Atlantic rhodolith bed. *J. Mar. Biol. Ass.* **2020**, *100*, 347–360. [CrossRef]
53. Dickson, A.; Sabine, C.L.; Christian, J. *Guide to Best Practices for Ocean CO2 Measurement*; PICES Special Publication; PICES, 2007.
54. Bernal, C.; Sánchez-Cabeza, J.A.; Martínez-Galarza, R.A.; Gómez, M.; Norzagaray-López, O. *Determinación de Carbono Inorgánico Disuelto en Agua de Mar Utilizando Analizador Automático con Detección Infrarrojo—AIRICA.*; REMARCO: Santa Marta, Colombia, 2021; 18p, Available online: https://remarco.org/manual-ao/ (accessed on 15 March 2022).
55. Pierrot, D.; Lewis, E.; Wallace, D. *MS Excel Program Developed for CO_2 System Calculations. ORNL/CDIAC-105a*; Carbon Dioxide Information Analysis Center, Oak Ridge National Laboratory, U.S. Department of Energy: Oak Ridge, TN, USA, 2006.
56. Mehrbach, C.; Culberson, C.H.; Hawley, J.E.; Pytkowicx, R.M. Measurement of the apparent dissociation constants of carbonic acid in seawater at atmospheric pressure. *Limnol. Oceanogr.* **1973**, *18*, 897–907. [CrossRef]
57. Dickson, A.G.; Millero, F.J. A comparison of the equilibrium constants for the dissociation of carbonic acid in seawater media. *Deep-Sea Res.* **1987**, *34*, 1733–1743. [CrossRef]
58. Leuker, T.J.; Dickson, A.G.; Keeling, C.D. Ocean pCO_2 calculated from dissolved inorganic carbon, alkalinity, and equations for K1 and K2. Validation based on laboratory measurements of CO_2 in gas and seawater at equilibrium. *Mar. Chem.* **2000**, *70*, 105–119. [CrossRef]
59. Dickson, A.G. Thermodynamics of the dissociation of boric acid in synthetic seawater from 273.15 to 318.15 K. *Deep Sea Res. Part A. Oceanogr. Res. Pap.* **1990**, *37*, 755–766. [CrossRef]
60. Lee, K.; Millero, F.J.; Byrne, R.H.; Feely, R.A.; Wanninkhof, R. The recommended dissociation constants for carbonic acid in seawater. *Geophys. Res. Lett.* **2000**, *27*, 229–232. [CrossRef]
61. Smith, S.V.; Key, G.S. Carbon dioxide and metabolism in marine environments1. *Limnol. Oceanogr.* **1975**, *20*, 493–495. [CrossRef]
62. Chisholm, J.R.M.; Gattuso, J.-P. Validation of the alkalinity anomaly technique for investigating calcification and photosynthesis in coral reef communities. *Limnol. Oceanogr.* **1991**, *36*, 1232–1239. [CrossRef]
63. Fajardo, G. Surgencia costera en las proximidades de la península colombiana de La Guajira. *Bol. Cien. CIOH* **1979**, *2*, 7–10. [CrossRef]
64. Ávila-Melean, R. Dióxido de carbono total y su relación con el oxígeno disuelto en las aguas del Golfo de Santa Fe, Estado Sucre, Venezuela. *Bol. Inst. Oceanogr. Univ. Oriente* **1976**, *15*, 133–139.
65. Zhang, J.Z.; Millero, F.J. The chemistry of the anoxic waters in the Cariaco Trench. *Deep-Sea Res.* **1993**, *40*, 1023–1041. [CrossRef]
66. Astor, Y.M.; Lorenzoni, L.; Thunell, R.; Varela, R.; Muller-Karger, F.; Troccoli, L.; Taylor, G.T.; Scranton, M.I.; Tappa, E.; Rueda, D. Interannual variability in sea surface temperature and fCO_2 changes in the Cariaco Basin. *Deep Sea Res. Part II Top. Stud. Oceanogr.* **2013**, *93*, 33–43. [CrossRef]
67. Hernández-Guerra, A.; Joyce, T.M. Water masses and circulation in the surface layers of the Caribbean at 66°W. *Geophys. Res. Lett.* **2000**, *27*, 3497–3500. [CrossRef]
68. Anthony, K.R.N.; Kleypas, J.; Gattuso, J.-P. Coral reefs modify their seawater carbon chemistry—Implications for impacts of ocean acidification. *Glob. Change Biol.* **2011**, *17*, 3655–3666. [CrossRef]
69. Cyronak, T.; Andersson, A.J.; Langdon, C.; Albright, R.; Bates, N.R.; Caldeira, K.; Carlton, R.; Corredor, J.E.; Dunbar, R.B.; Enochs, I.; et al. Taking the metabolic pulse of the world's coral reefs. *PLoS ONE* **2018**, *13*, e0190872. [CrossRef] [PubMed]
70. Marubini, F.; Ferrier–Pages, C.; Cuif, J. Suppression of skeletal growth in scleractinian corals by decreasing ambient carbonate-ion concentration: A cross-family comparison. *Proc. R. Soc. Lond. B* **2003**, *270*, 179–184. [CrossRef] [PubMed]
71. Glynn, P.W. Coral growth in upwelling and nonupwelling areas off the Pacific coast of Panamá. *J. Mar. Res.* **1977**, *35*, 567–585.
72. Porter, J.W.; Battey, J.F.; Smith, G.J. Perturbation and change in coral reef communities. *Proc. Natl. Acad. Sci. USA* **1982**, *79*, 1678–1681. [CrossRef]
73. Saxby, T.; Dennison, W.; Hoegh-Guldberg, O. Photosynthetic responses of the coral *Montipora digitata* to cold temperature stress. *Mar. Ecol. Prog. Ser.* **2003**, *248*, 85–97. [CrossRef]
74. Schneider, K.; Erez, J. The effect of carbonate chemistry on calcification and photosynthesis in the hermatypic coral *Acropora eurystoma*. *Limnol. Oceanogr.* **2006**, *51*, 1284–1293. [CrossRef]
75. Steller, D.; Hernandez-Ayón, J.; Riosmena-Rodríguez, R.; Cabello-Pasini, A. Effect of temperature on photosynthesis, growth and calcification rates of the free-living coralline alga *Lithophyllum margaritae*. *Cienc. Mar.* **2007**, *33*, 441–456. [CrossRef]
76. de Putron, S.J.; McCorkle, D.C.; Cohen, A.L.; Dillon, A.B. The impact of seawater saturation state and bicarbonate ion concentration on calcification by new recruits of two Atlantic corals. *Coral Reefs* **2011**, *30*, 321–328. [CrossRef]

77. Marubini, F.; Thake, B. Bicarbonate addition promotes coral growth. *Limnol. Oceanogr.* **1999**, *44*, 716–720. [CrossRef]
78. Herfort, L.; Thake, B.; Taubner, I. Bicarbonate stimulation of calcification and photosynthesis in two hermatypic corals. *J. Phycol.* **2008**, *44*, 91–98. [CrossRef]
79. Okazaki, R.R.; Swart, P.K.; Langdon, C. Stress-tolerant corals of Florida Bay are vulnerable to ocean acidification. *Coral Reefs* **2013**, *32*, 671–683. [CrossRef]
80. Roberty, S.; Béraud, E.; Grover, R.; Ferrier-Pagès, C. Coral productivity is co-limited by bicarbonate and ammonium availability. *Microorganisms* **2020**, *8*, 640. [CrossRef] [PubMed]
81. Acosta-Chaparro, A.; González, J.D.; Navas-Camacho, R.; Sánchez, L. *Estado de las Formaciones Coralinas del Parque Nacional Natural Tayrona*; Informe Técnico de Monitoreo Ecosistémico ITF#2; Invemar: Santa Marta, Colombia, 2018; 55p.
82. Chollett, I.; Mumby, P.J.; Cortés, J. Upwelling areas do not guarantee refuge for coral reefs in a warming ocean. *Mar. Ecol. Prog. Ser.* **2010**, *416*, 47–56. [CrossRef]
83. Sawall, Y.; Harris, M.; Lebrato, M.; Wall, M.; Feng, E.Y. Discrete pulses of cooler deep water can decelerate coral bleaching during thermal stress: Implications for artificial upwelling during heat-stress events. *Front. Mar. Sci.* **2020**, *7*, 720. [CrossRef]
84. Arias-González, J.E.; Baums, I.B.; Banaszak, A.T.; Prada, C.; Rossi, S.; Hernández-Delgado, E.A.; Rinkevich, B. Editorial: Coral reef restoration in a changing world: Science-based solutions. *Front. Mar. Sci.* **2022**, *9*, 919603. [CrossRef]